Diamond & Related Materials 36 (2013) 35–43

Contents lists available at SciVerse ScienceDirect

Diamond & Related Materials

journal homepage: www.elsevier.com/locate/diamond

Influence of boron on donor–acceptor pair recombination in type IIa HPHT diamonds

Patrik Ščajev [a,*], Laima Trinkler [b], Baiba Berzina [b], Eugeny Ivakin [c], Kęstutis Jarašiūnas [a]

[a] Institute of Applied Research, Vilnius University, Saulėtekio Ave. 9 — III, Vilnius 10222, Lithuania
[b] Institute of Solid State Physics, University of Latvia, Kengaraga 8, 1063 Riga, Latvia
[c] Institute of Physics, Academy of Sciences of Belarus, Nazaleznosti Ave. 68, 220072 Minsk, Belarus

ARTICLE INFO

Article history:
Received 31 December 2012
Received in revised form 28 March 2013
Accepted 31 March 2013
Available online 18 April 2013

Keywords:
HPHT diamond
Photoluminescence
Donor–acceptor recombination
Two photon absorption
Differential transmittivity
Activation energy

ABSTRACT

We report on the investigation of donor–acceptor pair (DAP) and free carrier recombination in HPHT IIa type diamonds and determination of boron concentration by differential transmittivity (DT) technique. Photoluminescence and photoluminescence excitation spectra were measured in 8–300 K temperature range and provided a broad (~0.67 eV) Gaussian DAP band which peaked at 2.2 eV at low temperatures, while above 200 K it sharply shifted to 2.5 eV and became more intense. Thermoluminescence measurements also demonstrated a similar tendency. This peculiarity was explained by DAP recombination between the nitrogen and the boron, the latter being in the ground and the excited states at low and high temperatures, respectively. A zero phonon line position coincided with the calculated one, when using nitrogen and boron activation energies. Scanning of DT across the sample at different delay times revealed the fast (200–500 ns) free carrier lifetime and the slow recovery time (of optically recharged boron to its initial state). The temperature dependence of the slow component decay time provided the boron activation energy of 360 meV. Saturation of the boron-related DT signal in the samples and the determined boron ionization cross section at 1064 nm ($\sigma_B = 3.3 \times 10^{-17}$ cm^2) provided the boron density in $10^{14–16}$ cm^{-3} range and revealed its strongly inhomogeneous distribution across the HPHT layers. The B density was found much lower than the density of nitrogen donors (~10^{17} cm^{-3}), which were distributed in the layers much more homogeneously.

1. Introduction

Diamond is a very prospective opto-electronic material due to its outstanding mechanical, thermal and electrical properties [1], however huge variety of optically active defect centers makes it difficult to distinguish them and evaluate their impact on these properties. Therefore we analyze the most active defects in high quality HPHT diamonds, namely the nitrogen and the boron. The nitrogen (~1.8 eV [2]) is known to be the lifetime limiting defect [3–7], while boron (0.37 eV [1,2]) is the p-type dopant and a compensating center [8,9]. We evaluated nitrogen impact on carrier lifetime by measuring differential transmittivity (DT) decay [10] under two photon carrier excitation (nitrogen density was determined from optical absorption spectra). It is widely debated in literature about the origin of the luminescence in natural and HPHT synthetic diamonds due to abundance of defects having similar emission bands and their unambiguous assignment [8]. The most prominent feature is a band peaking at 2.5 eV, called the A band [2,8,11]. Only this band was observed in our samples and was extensively analyzed. In literature it is attributed to nitrogen donor to boron acceptor recombination. The involvement of nitrogen in this process was verified in [12], while boron impact was still under debates. In the [13–16] two bands at 2.2 (at low temperatures) and 2.5 eV (at high temperatures) were observed by cathodo- and photo-luminescence, while clear interpretation of their origin has not been provided. We conclude that these two bands are related to the same boron acceptor at its ground and excited states. A proof that boron acceptor is present in the samples was provided by determination of boron activation energy from the measured DT recovery time. Direct correlation of photoluminescence intensity with lateral boron concentration also confirmed this assumption.

2. Samples and experimental techniques

We investigated two IIa type HPHT samples H1 and H2 (of thicknesses d = 1.0 and 1.1 mm, respectively; grown in a system with temperature gradient and nitrogen getter). The samples were provided by the Institute for Superhard Materials of the National Academy of Sciences of Ukraine. Photoluminescence studies were performed on H1, while DT kinetics due to recharged boron were measured in boron-rich sample H2. According to [17] in the central part of the samples neutral nitrogen densities were $N^0 = 4.3 \times 10^{16}$ and 1.1×10^{17} cm^{-3}, while the ionized nitrogen densities were quite similar: $N^+ = 2.1 \times 10^{16}$ cm^{-3} and 2.6×10^{16} cm^{-3}, indicating nitrogen compensation by acceptors (tentatively nitrogen aggregates). Already large amount ($2;4 \times 10^{17}$ cm^{-3}) of hydrogen was present in the samples; however hydrogen is probably not active as acceptor, but working as a bond passivation center [18].

* Corresponding author. Tel.: +370 5 2366036; fax: +370 5 2366037.
E-mail address: patrik.scajev@ff.vu.lt (P. Ščajev).

0925-9635/$ – see front matter © 2013 Elsevier B.V. All rights reserved.
http://dx.doi.org/10.1016/j.diamond.2013.03.011

The photoluminescence emission (PL) and photoluminescence excitation (PLE) spectra of the samples were measured using a setup for spectral measurements equipped with a deuterium lamp LDD-400 as a source of UV light and a grating monochromator MDR-2 in the excitation channel [19]. In the case of PLE measurements the luminescence signal was analyzed with a prism monochromator SPM-2 and detected with a Hamamatsu photomultiplier tube H 7468–20. PLE spectra were corrected for the apparatus spectral response. In the case of the PL and thermoluminescence (TL) emission measurements the luminescence signal was analyzed by an Andor monochromator SR-303i-B using a grating with 150 lines/mm and 500 nm blaze, and detected with a CCD camera DV420A-BU2 in the accumulation mode. The spectral resolution was 10–20 meV. The low temperature measurements were fulfilled using a closed cycle helium refrigerator Janis, which allowed achieving sample temperature in 8–300 K range.

The DT measurements were performed using UV excitation and IR probing. For carrier injection, a Nd:YLF laser (operating at $\lambda_1 =$ 1053 nm with 10 Hz repetition rate and pulse duration of $\tau_{1h} =$ 15 ps) was used. Its 3-rd harmonic pulse at $\lambda_3 = 351$ nm generated the carriers in the bulk via two photon (2P) interband transitions [20], providing their density in $10^{15} - 3 \times 10^{17}$ cm^{-3} range. Interband carrier generation at $\lambda_5 = 213$ nm wavelength (the 5-th harmonic of Nd:YAG laser, $\tau_{1h} = 25$ ps) generated carriers in a 3-μm thick surface region and allowed to calculate their lifetimes on the surfaces. The optically delayed (<4 ns) picosecond probe pulse at $\lambda_1 = 1053$ nm was used to monitor the fast decay transients. For measurement of longer relaxation tails (>5 ns), an electronically delayed ~2 ns duration probe pulse at 1064 nm was generated from a diode-pumped Nd:YAG laser, triggered by a Nd:YLF laser [10]. Even slower decays (>0.1 s) were measured using a single excitation pulse and subsequent detection of sample transmission with 10 Hz repetition rate to full signal extinction. Temperature was controlled in 80–300 K range, placing the sample in nitrogen cryostat from CRYO Industries. For measurements of lifetime variation across the sample, it was mounted on a translation stage and DT signal scans were performed at different probe beam delays. The probe diameter of 50 μm was used, being much smaller than the pump diameter (360 μm).

3. Results and discussion

3.1. Absorption spectra

The optical excitation mechanisms can be separated to intrinsic interband electron–hole pair generation [21], when absorbed quantum energy is higher than the bandgap E_g, while for lower quanta absorption by defects dominates (usually by nitrogen and boron in case of diamond [8]). These two types of absorption in the studied samples are analyzed in this section. The absorption spectra of the investigated samples were taken from [17] and fitted in order to separate different transitions, involving nitrogen and interband ones. This procedure is needed for PLE spectra interpretation.

Intrinsic band-to-band absorption (BBA) coefficient temperature and quantum energy E (in electronvolts, eV) dependence in diamond can be approximated using temperature dependent excitonic bandgap $E_{GX}(T)$, absorption strength A, exciton binding energy $E_{ex} = 80$ meV [22] and phonon energy E_{ph} [23–25]:

$$\alpha_{BBA}(T) = \frac{n_B + 1/2 \pm 1/2}{E}\left[\sum_i A_{exc,i}\left(E - \left(E_{GX}(T) \pm iE_{ph}\right)\right)^{1/2} + A_{IB}\left(E - \left(E_{GX}(T) \pm E_{ph} + E_{ex}\right)\right)^2\right]. \quad (1)$$

Here "+" sign corresponds to phonon emission, the "–" sign for absorption, $n_B = (\exp(E_{ph}/kT) - 1)$ is the Bose–Einstein phonon population factor. The first term in the brackets corresponds to excitonic, while the second one for free carrier interband absorption. We considered multiple phonon absorption by excitons (i = 1,2,3,4,…) with phonon energy $E_{ph} \approx 70$ meV [26]. The bandgap changes very weakly in 8–300 K range [26,27] and its impact of 10–20 meV [26] is almost compensated by thermal broadening (~26 meV at RT). The stronger impact on absorption spectra comes from the increase of phonon-assisted absorption with temperature.

The absorption spectra with relevant fits are provided on Fig. 1. For BBA fitting we used the following parameters: $A_{IB} = 1.9 \times 10^5$ cm^{-1} eV^{-1}, $E_{ph} = 68$ meV, $E_{GX} = 5.44$ eV, $A_{exc,i} = 707$, 990, 283, 23 cm^{-1} eV$^{1/2}$, and i = 1,2,3,4. The bandgap value rather well coincides with the literature value of 5.46 eV at RT (5.48 eV at 8 K) [27]. The rigid bandgap $E_G = (E_{GX} + E_{ex}) = 5.52$ eV was calculated. Total sum fits of all absorption processes (Fig. 1b) rather well

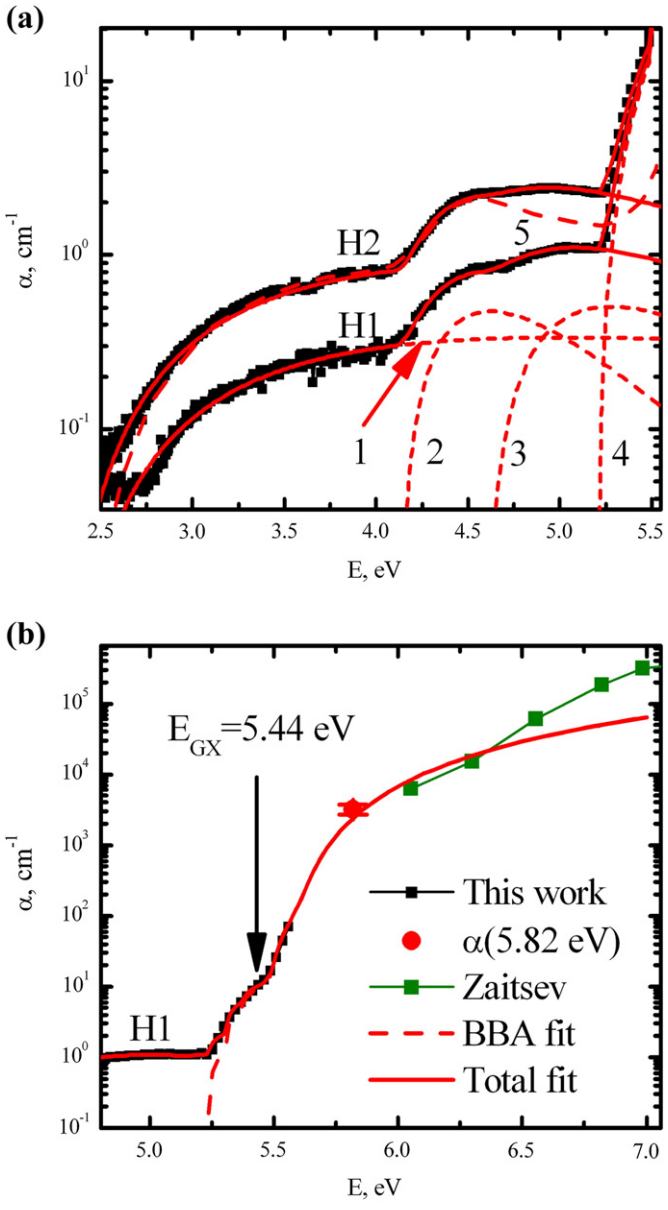

Fig. 1. Absorption spectra of the investigated diamond layers H1and H2 in the spectral regions below the bandgap (a) and in the vicinity of absorption edge (b). In (a) the dashed lines 1 to 3 designate nitrogen transitions $N^0 \rightarrow N^+$, $N^0 \rightarrow N^-$ and $N^+ \rightarrow N^0$, respectively. The line 4 is the band-to-band absorption (BBA) component. The line 5 is the absorption spectrum (normalized by 150 factor) of a heavily nitrogen-doped layer ($N^0 = 1.8 \times 10^{19}$ cm^{-3} [30], with low compensation). Solid curves are the total absorption fits. In (b), the BBA fit is given using data from Ref. [8]. The absorption coefficient value of 3×10^3 cm^{-1} at the used excitation quantum energy of 5.82 eV (a full circle) was determined by us using a diffraction based technique [32].